

Oxygen at high pressures: a theoretical approach to monoatomic phases

This article has been downloaded from IOPscience. Please scroll down to see the full text article.

2007 *J. Phys.: Condens. Matter* 19 365211

(<http://iopscience.iop.org/0953-8984/19/36/365211>)

[View the table of contents for this issue](#), or go to the [journal homepage](#) for more

Download details:

IP Address: 129.252.86.83

The article was downloaded on 29/05/2010 at 04:37

Please note that [terms and conditions apply](#).

Oxygen at high pressures: a theoretical approach to monoatomic phases

T Oda¹, K Sugimori¹, H Nagao¹, I Hamada², S Kagayama³, M Geshi³, H Nagara³, K Kusakabe³ and N Suzuki³

¹ Graduate School of Natural Science and Technology, Kanazawa University, Kanazawa 920-1192, Japan

² Department of Condensed Matter Physics, The Institute of Scientific and Industrial Research (ISIR), Osaka University, 8-1 Mihogaoka, Ibaraki, Osaka 567-0047, Japan

³ Division of Material Physics, Department of Physical Science, Graduate School of Engineering Science, Osaka University, Toyonaka 560-8531, Japan

E-mail: oda@cphys.s.kanazawa-u.ac.jp

Received 2 December 2006, in final form 17 January 2007

Published 24 August 2007

Online at stacks.iop.org/JPhysCM/19/365211

Abstract

We have studied the ζ -phase of solid oxygen using the generalized gradient approximation in the density functional approach. Calculations of total energies and pressures have been carried out for the prototype of diatomic ζ -phase and other hypothetical monoatomic crystal structures. The diatomic phase was found to be stable over a wide range of pressure (100–2000 GPa). The stacking of molecular layers is discussed in comparison with the available experimental data.

1. Introduction

Oxygen consists of a diatomic magnetic molecule, which has a spin-triplet ground state under low pressures. This molecular magnetism is the main origin of the paramagnetic or antiferromagnetic properties of condensed oxygen. In the ε -phase, the quench of magnetic long range order was reported in spin-polarized neutron diffraction measurements [1]. Recently, the unique crystal structure of oxygen, the $(O_2)_4$ molecular lattice, has been determined in the ε -phase by Fujihisa *et al.* Their Rietveld analysis for the x-ray diffraction measurements in powder samples shows a much better fit compared with that of the previous structure model [2]. Results of the $(O_2)_4$ lattice have since been reported for single crystal samples [3]. This molecular picture at low pressures in the ε -phase gradually changes as pressure increases to a two-dimensional one which consists of aligned molecules. The structural phase transition to the ζ -phase has been observed at 96 GPa [4].

High pressures have induced in oxygen the appearance of metallic features. Superconducting properties were also reported around 100 GPa in ζ -phase [5]. Above the transition pressure, the existence of molecular vibrations has been indicated by Raman

measurements [6]. Serra *et al* found a prototype for the ζ -phase in a simulation starting from the structure of the δ -phase. At the phase transition, the sliding of molecular layers has been discussed in previous works [6, 7]. The structure proposed by Serra *et al* is consistent with maintaining a molecular form. The first x-ray measurements on powder samples reported six diffraction peaks at 116 GPa. For single crystal samples, Weck *et al* captured four diffraction angles at 110 GPa [6]. These angles contain the diffraction which showed only slight change and keeps the same angles. The two of four angles have been discussed in relation to the sliding of molecular layers.

As pressure increases to a high value, monoatomic phases would be expected, as observed in I_2 , Br_2 , Cl_2 [8–11]. Otani *et al* studied the monoatomic phases using a linearized muffin-tin orbital method and discussed the stability of the β -Po structure compared with bcc structure [12]. Neaton *et al* provided an enthalpy curve for the ζ -phase at pressures lower than 80 GPa [13].

To find a monoatomic phase of solid oxygen, we have studied the structural properties and stability of typical monoatomic and molecular phases in oxygen. We have calculated the enthalpy of crystal structures at zero temperature as a function of pressure. The diatomic ζ -phase is found to be stable over a wide range of pressures.

2. Method and crystal structures

For the density functional theory (DFT) [14] we used planewave basis to represent wavefunctions and electron densities and ultrasoft-type pseudopotentials [15, 16] to include core–valence interactions. The 1s states were included in the core, while the other states were described explicitly. In the construction of pseudopotentials, we took a cut-off radius of 0.609 Å including d-symmetry local orbitals [17]. Energy cut-offs of 100 and 400 Ryd were taken for the wavefunction and electron density, respectively. The exchange and correlation energy was treated in the generalized gradient approximation proposed by Perdew and Wang (PW91) [18]. We used the sets of special points for sampling \mathbf{k} points [19]. The ground state of the molecule corresponds to the spin-polarized state with a magnetization of $2 \mu_B$ and shows a bond length of 1.22 Å, a vibrational frequency of 46.7 THz and a binding energy of 5.99 eV. The former two are in good agreement with the corresponding experimental values (1.21 Å, 47.39 THz) and the latter is 17% larger than the experimental value (5.12 eV) [20]. These properties are similar to the previous results obtained in density functional approaches to oxygen [7, 13, 17].

The crystal structure of the ζ -phase has not been determined experimentally, but since Serra *et al* proposed an base-centred orthorhombic structure, presented by the space group of $C2mm$, it has been used as a prototype of the ζ -phase [13, 21]. Figure 1 present the crystal structure which we call the prototype in this paper. The parameters of the structure are a , b , c , v , f . The last parameter f specifies the bond length of the molecule. This prototype also implies that the aligned molecules form a triangular lattice in the ab -plane. This property is presented by the ratio of $b/a \sim 1/\sqrt{3}$. The prototype has hexagonal-closed-packed layer stacking for the c -direction. We also treated it a hexagonal lattice in our work. We also considered a cubic-closed-packed layer stacking for c -direction. This structure can be treated as a rhombohedral lattice.

For monoatomic crystal structures we considered the β -Po structure, as in the previous work [12]. It is convenient to investigate this structure because it contains typical simple structures (fcc, sc, bcc) in variations of lattice parameters. We also considered the hexagonal closed packing (hcp) and simple hexagonal (sh) structures. Because these structures have a much larger energy than the optimized structures in the β -Po structure, we do not present the results in this paper.

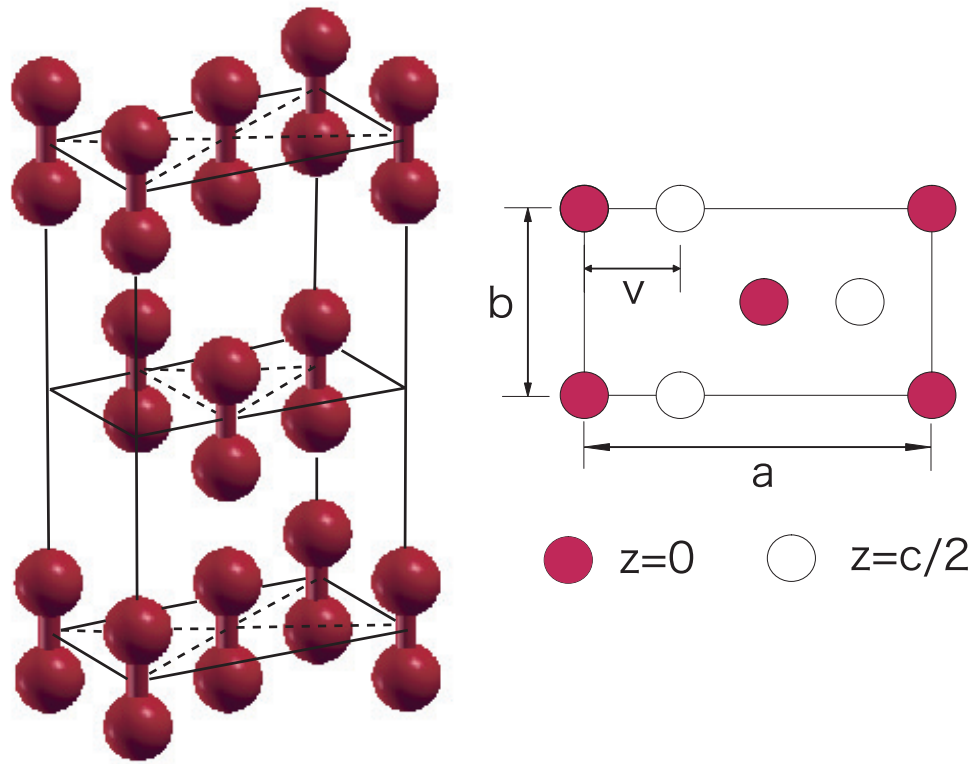


Figure 1. The prototype crystal structure for the ζ -phase, found by Serra *et al* [7].
(This figure is in colour only in the electronic version)

In this work we optimize the structural parameters by using calculated pressures and atomic forces. For a given pressure, the enthalpy is estimated with total energy (E), pressure (p) and volume (Ω); $H = E + p\Omega$. For the sampling \mathbf{k} points, we used a $12 \times 12 \times 10$ mesh for the prototype of the ζ -phase, and a $16 \times 16 \times 16$ mesh for the β -Po structure of the monoatomic phase. When we need an accuracy to total energies, we used the $26 \times 26 \times 26$ mesh for the trigonal system of a one-molecule unit cell and the $18 \times 18 \times 18$ mesh for the hexagonal system of a two-molecule unit cell. The above convergence amounts to 0.007 mHa/atom in the trigonal and 0.05 mHa/atom in the hexagonal at 1920 GPa. At lower pressures the accuracy would become higher.

3. Results and discussions

The monoatomic phase of β -Po structure has two lattice parameters. Figure 2 presents the total energies for various parameters, volume (Ω) and cosine of the trigonal angle ($\cos \alpha_r$). At larger volumes (low pressures), simple cubic (sc) structures, having $\cos \alpha_r = 0$, have the lowest energy. At smaller volumes, the lowest energy state changes to the β -Po structure which has $\cos \alpha_r$ of -0.20 to -0.25 (β -Po-I). The body centred cubic (bcc) structure does not take a lowest energy state for the volume range of 2.50 – 6.40 \AA^3 /atom. The semi-stable state appears at $\cos \alpha_r$ of -0.40 to -0.43 (β -Po-II). Our result described above is similar to

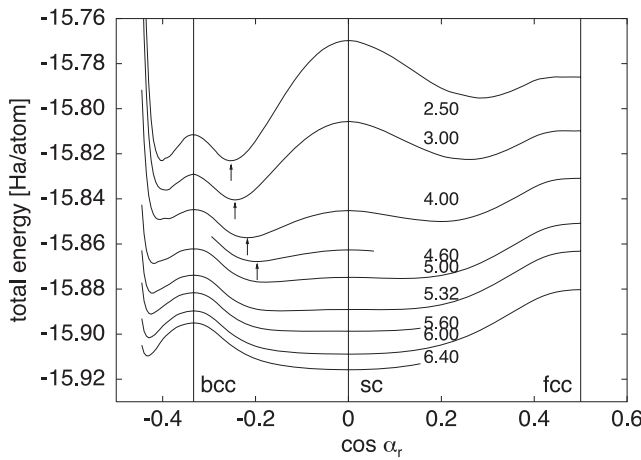


Figure 2. Total energy E of β -Po structures as a function of lattice parameter, $\cos \alpha_r$, where α_r is the angle between the pair of trigonal axes. The curve specifies a variation for a fixed volume and the curves are shifted to downward to draw them in the same figure; shifted by 0.012, 0.050, 0.200, 0.350 Ha for $\Omega = 4.60, 4.00, 3.00, 2.50 \text{ \AA}^3/\text{atom}$. The arrows point at the minima of E for a given volume.

that of previous work [12] corresponding to a more qualified version of the β -Po structure. In our work, pressures are also calculated and the results are compared with the prototype of diatomic phases in enthalpy, as presented later.

The prototype structure of the ζ -phase was found to be stable over a wide range of pressures. In figure 3, the enthalpy as a function of pressure is presented for the prototype of the ζ -phase, compared with sc and β -Po-I, at pressures up to 2000 GPa. The prototype of the ζ -phase is much lower in enthalpy than the β -Po-I of the monoatomic phase. The bond length of molecules (1.180 Å at 114 GPa) is gradually decreased to 1.034 Å at 1920 GPa. The atomic distances between molecular layers are 2.193, 1.589 Å for 114 and 1920 GPa, respectively. These are still far from intramolecular bond lengths. The stability of the prototype might be attributed to close packing of molecules in the ab -plane, as well as formation of molecular bonds. Indeed, the structure parameters obtained for the prototype show that $b/a \sim 0.57$ and $v/a \sim 0.33$ at all pressures we investigated. Our results are consistent with those of the work by Serra *et al* [7], in which the lattice parameters ($a, b, c = 3.62, 2.10, 6.11 \text{ \AA}$ at 116 GPa) are similar to ours ($a, b, c = 3.63, 2.10, 6.02 \text{ \AA}$ at 114 GPa).

We also calculated the enthalpy of a two-molecule unit cell with the hexagonal constraint, obtaining a similar enthalpy to that for the structure of $C2mm$. We considered another structure with an ABC stacking along the c -direction (the trigonal structure), while the prototype has an AB stacking. The molecular layer of O_2 in the ab -planes would be rigid, and it is interesting to compare energies for the sequence of stacking to access the structure of the ζ -phase. The sliding of layers inferred at the phase transition from the ε -phase to the ζ -phase encourages an investigation of the stacking of molecular layers. In figure 4 the energy differences are presented. At high pressures the enthalpy of the trigonal structure is slightly lower than that of the hexagonal one. However, the differences are only a few factors of the accuracy of \mathbf{k} -point sampling.

The stacking of molecular layers causes the diffraction peaks which correspond to the spacings of the layers. In the calculated structures at 114 GPa, the spacings of the layers (d_0) are 3.009 and 3.010 Å for hexagonal and trigonal structures, respectively, which compare to the values (2.9858 Å [6], 2.9852 Å [4]) from the experiments. The calculated values are larger

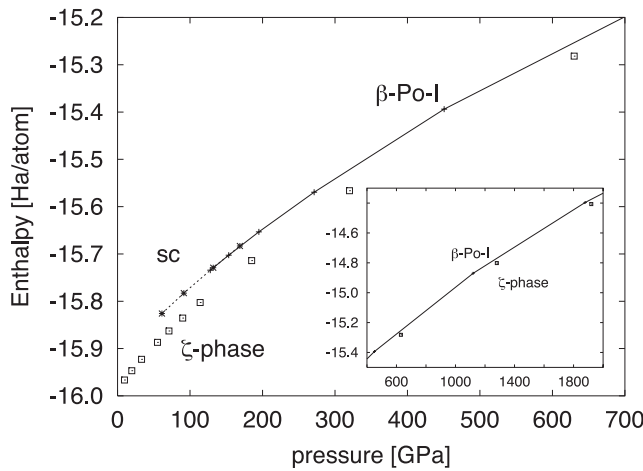


Figure 3. Enthalpy as a function of pressure in the oxygen of high-pressure structures; β -Po structure (plus), simple cubic structure (star) and the prototype of ζ -phase (box).

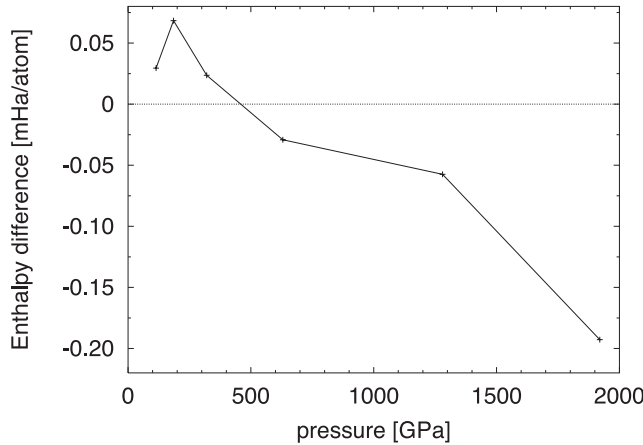


Figure 4. The enthalpy of the diatomic trigonal structure with respect to that of the diatomic hexagonal structure.

by 0.8% than the experimental ones, which shows the typical accuracy of the DFT approach. The lattice constant in the ab -planes (a_{hex}) is estimated to be 2.098 and 2.099 Å at 114 GPa.

Some of diffraction angles in the trigonal structure coincide with the observed diffraction angles in the ζ -phase. For the hexagonal and trigonal structures, the diffraction angles are calculated using the formula for the reciprocal lattice vectors are given in table 1. In this table, only those reciprocal lattice vectors which are expected to provide larger peaks in x-ray diffraction measurements are listed. The diffraction angles are summarized in table 2, compared with the result of the x-ray diffraction measurement for single crystal samples [6]. The pairs of \vec{G}_{11} and \vec{G}_{12} , for example, form the couple of angles. As seen in table 2, the three experimental values would correspond to the angles from the trigonal structure. The fact that the diffraction peaks from \vec{G}_{11} and \vec{G}_{12} are identified as the diffractions which have been related to the sliding of molecular layers at the phase transition in the experiment [6], largely supports the appearance of ABC stacking of layers instead of a hexagonal (AB) one in the ζ -phase.

Table 1. The reciprocal lattice vectors whose diffractions provide relatively large peaks in the hexagonal and trigonal structures. a_{hex} and d_0 ($\equiv c_{\text{hex}}/2$) are the lattice parameter of the triangular lattice and the distance of molecular layers, respectively. The opposite directions of the listed vectors should be added to obtain the full representation.

Hexagonal	Trigonal
$\vec{G}_{\text{h}0}(002) = \frac{2\pi}{d_0} \vec{e}_z$	$\vec{G}_{\text{t}0}(111) = \frac{2\pi}{d_0} \vec{e}_z$
$\vec{G}_{\text{h}1}(010) = \frac{2\sqrt{3}}{3} \frac{2\pi}{a_{\text{hex}}} \vec{e}_y$	$\vec{G}_{\text{t}1}(100) = \frac{2\pi}{a_{\text{hex}}} \vec{e}_x + \frac{\sqrt{3}}{3} \frac{2\pi}{a_{\text{hex}}} \vec{e}_y + \frac{2}{3} \frac{2\pi}{2d_0} \vec{e}_z$
$\vec{G}_{\text{h}1}(1\bar{1}0) = \frac{2\pi}{a_{\text{hex}}} \vec{e}_x - \frac{\sqrt{3}}{3} \frac{2\pi}{a_{\text{hex}}} \vec{e}_y$	$\vec{G}_{\text{t}1}(010) = -\frac{2\pi}{a_{\text{hex}}} \vec{e}_x + \frac{\sqrt{3}}{3} \frac{2\pi}{a_{\text{hex}}} \vec{e}_y + \frac{2}{3} \frac{2\pi}{2d_0} \vec{e}_z$
$\vec{G}_{\text{h}1}(100) = \frac{2\pi}{a_{\text{hex}}} \vec{e}_x + \frac{\sqrt{3}}{3} \frac{2\pi}{a_{\text{hex}}} \vec{e}_y$	$\vec{G}_{\text{t}1}(001) = -\frac{2\sqrt{3}}{3} \frac{2\pi}{a_{\text{hex}}} \vec{e}_y + \frac{2}{3} \frac{2\pi}{2d_0} \vec{e}_z$
$\vec{G}_{\text{h}2}(011) = \frac{2\sqrt{3}}{3} \frac{2\pi}{a_{\text{hex}}} \vec{e}_y + \frac{2\pi}{2d_0} \vec{e}_z$	$\vec{G}_{\text{t}2}(011) = -\frac{2\pi}{a_{\text{hex}}} \vec{e}_x - \frac{\sqrt{3}}{3} \frac{2\pi}{a_{\text{hex}}} \vec{e}_y + \frac{4}{3} \frac{2\pi}{2d_0} \vec{e}_z$
$\vec{G}_{\text{h}2}(01\bar{1}) = \frac{2\sqrt{3}}{3} \frac{2\pi}{a_{\text{hex}}} \vec{e}_y - \frac{2\pi}{2d_0} \vec{e}_z$	$\vec{G}_{\text{t}2}(101) = \frac{2\pi}{a_{\text{hex}}} \vec{e}_x - \frac{\sqrt{3}}{3} \frac{2\pi}{a_{\text{hex}}} \vec{e}_y + \frac{4}{3} \frac{2\pi}{2d_0} \vec{e}_z$
$\vec{G}_{\text{h}2}(1\bar{1}1) = \frac{2\pi}{a_{\text{hex}}} \vec{e}_x - \frac{\sqrt{3}}{3} \frac{2\pi}{a_{\text{hex}}} \vec{e}_y + \frac{2\pi}{2d_0} \vec{e}_z$	$\vec{G}_{\text{t}2}(110) = \frac{2\sqrt{3}}{3} \frac{2\pi}{a_{\text{hex}}} \vec{e}_y + \frac{4}{3} \frac{2\pi}{2d_0} \vec{e}_z$
$\vec{G}_{\text{h}2}(1\bar{1}\bar{1}) = \frac{2\pi}{a_{\text{hex}}} \vec{e}_x - \frac{\sqrt{3}}{3} \frac{2\pi}{a_{\text{hex}}} \vec{e}_y - \frac{2\pi}{2d_0} \vec{e}_z$	
$\vec{G}_{\text{h}2}(101) = \frac{2\pi}{a_{\text{hex}}} \vec{e}_x + \frac{\sqrt{3}}{3} \frac{2\pi}{a_{\text{hex}}} \vec{e}_y + \frac{2\pi}{2d_0} \vec{e}_z$	
$\vec{G}_{\text{h}2}(10\bar{1}) = \frac{2\pi}{a_{\text{hex}}} \vec{e}_x + \frac{\sqrt{3}}{3} \frac{2\pi}{a_{\text{hex}}} \vec{e}_y - \frac{2\pi}{2d_0} \vec{e}_z$	

Table 2. The angles (in degrees) between the diffraction planes at 114 GPa. $\theta_{s,s'}$ specifies the angle between the reciprocal lattice vectors, \vec{G}_s and $\vec{G}_{s'}$. The experimental data in parentheses are compiled from table 1 in [6]. In the last row, the angles are listed, assuming the lattice parameters ($a_{\text{hex}} = 2.1297 \text{ \AA}$, $d_0 = 2.9858 \text{ \AA}$).

	$\theta_{\text{h}0,\text{h}1}$	$\theta_{\text{h}0,\text{h}2}$	$\theta_{\text{h}1,\text{h}2}$	$\theta_{\text{t}0,\text{t}1}$	$\theta_{\text{t}0,\text{t}2}$	$\theta_{\text{t}1,\text{t}2}$	Others
Calc.	90	73.2	16.8, 56.4	78.6	68.1	33.3, 58.1	
(Exp.)				(78.5)	(67.2)	(34.3)	(60.7)(61.5)(77.7)
Parameter	90	72.8	17.2, 56.5	78.4	67.6	34.0, 58.0	

Table 3. The d spacings (in \AA) of the diffraction planes for the trigonal structure at 114 GPa, compared with the experimental data at 116 and 110 GPa [4, 6].

	$d_{\text{t}0}$	$d_{\text{t}1}$	$d_{\text{t}2}$	$d_{\text{u}1}$	$d_{\text{u}2}$
Cal.	3.01	1.78	1.69		
Weck <i>et al</i>	2.9858	1.7819	1.6946		1.8444
Akahama <i>et al</i>	2.9852	1.7782	1.7119	1.9752	1.8601

For the trigonal structure, the d spacings of the diffraction planes are listed in table 3, compared with the experimental values. The calculated d spacings agree with the experimental values, while the couple of d spacings in experiments remains unresolved (called $d_{\text{u}1}$ and $d_{\text{u}2}$ in this work). The diffraction of $d_{\text{u}2}$ has been observed in both powder and single crystal samples. The value of $d_{\text{u}2}$ is similar to the value of $d_{\text{h}1}$. In the last row of table 2 we list the angles when we assume $a_{\text{hex}} = 2.1297 \text{ \AA}$ ($= 2\sqrt{3}d_{\text{u}2}/3$) and $d_0 = 2.9858 \text{ \AA}$. The series of trigonals is consistent with the experimental data. However, the diffraction angle from the $\vec{G}_{\text{t}0}(111)$ (normal to the molecular plane) is estimated to be 60.7° in the experiment, being inconsistent with $\theta_{\text{h}1,\text{t}0} = 90^\circ$.

The ABC stacking of molecular layers may explain some of the structural properties of the ζ -phase. However, a full understanding of the structure is still far off. The diffractions of $d_{\text{u}1}$

and d_{u2} do not show any drastic change at the phase transition unlike the d_{t1} and d_{t2} diffractions. That of $\theta_{t1,t2}$ has not yet been observed. The intraplanar atomic position would need to be determined to solve the crystal structure in the high pressure phase.

4. Summary

We have investigated the high pressure phases of oxygen in the range between 100 and 2000 GPa. The monoatomic phases, which have β -Po structures, are not lower in energy than the prototype of the diatomic ζ -phase. This implies that diatomic structures are stable over a wide range of pressures. The enthalpy calculations for the ABC and AB stackings of molecular layers show that the former is slightly more stable than the latter at high pressures. It was found from the angle analysis between diffraction planes that the ABC stacking was more favourable than the AB stacking, compared with the available experimental data.

Acknowledgments

The calculation in this work was carried out using the facilities of the Supercomputer Center, Institute for Solid State Physics, University of Tokyo. The authors have been partially supported by a Grant-in-Aid for Scientific Research in Priority Areas, Development of New Quantum Simulators and Quantum Design (nos. 17064009 and 17064013), of The Ministry of Education, Culture, Sports, Science, and Technology, Japan. One of the authors (TO) would like to thank the Japan Society for the Promotion of Science for financial support (no. 17510097).

References

- [1] Goncharenko I N 2005 *Phys. Rev. Lett.* **94** 205701
- [2] Fujihisa H, Akahama Y, Kawamura H, Ohishi Y, Shimomura O, Yamawaki H, Sakashita M, Gotoh Y, Takeya S and Honda K 2006 *Phys. Rev. Lett.* **97** 085503
- [3] Lundsgaard L F, Weck G, McMahon M I, Desgreniers S and Loubeyre P 2006 *Nature* **443** 201
- [4] Akahama Y, Kawamura H, Häusermann D, Hanfland M and Shimomura O 1995 *Phys. Rev. Lett.* **74** 4690
- [5] Shimizu K, Suhara K, Ikumo M, Eremets M I and Amaya K 1998 *Nature* **393** 767
- [6] Weck G, Loubeyre P and LeToullec R 2002 *Phys. Rev. Lett.* **88** 035504
- [7] Serra S, Chiarotti G, Scandolo S and Tosatti E 1998 *Phys. Rev. Lett.* **80** 5160
- [8] Takemura K, Minomura S, Shimomura O and Fuji Y 1980 *Phys. Rev. Lett.* **45** 1881
- [9] Takemura K, Sato K, Fujihisa H and Onoda M 2003 *Nature* **423** 971
- [10] Fujii Y, Hase K, Ohishi Y, Fujihisa H and Hamaya N 1989 *Phys. Rev. Lett.* **63** 536
- [11] Fujihisa H, Fujii Y, Takemura K and Shimomura O 1995 *J. Phys. Chem. Solids* **56** 1439
- [12] Otani M, Yamaguchi K, Miyagi H and Suzuki N 1998 *Rev. High Pressures Sci. Technol.* **7** 178
- [13] Neaton J B and Ashcroft N W 2002 *Phys. Rev. Lett.* **88** 205503
- [14] Hohenberg H and Kohn W 1964 *Phys. Rev.* **136** B864
Kohn W and Sham L J 1965 *Phys. Rev.* **140** A1133
- [15] Vanderbilt D 1990 *Phys. Rev. B* **41** 7892
- [16] Pasquarello A, Laasonen K, Car R, Lee C and Vanderbilt D 1992 *Phys. Rev. Lett.* **69** 1982
Laasonen K, Pasquarello A, Car R, Lee C and Vanderbilt D 1993 *Phys. Rev. B* **47** 10142
- [17] Militzer B, Gygi F and Galli G 2003 *Phys. Rev. Lett.* **91** 265503
- [18] Perdew J P, Chevary J A, Vosko S H, Jackson K A, Pederson M R, Singh D J and Fiolhais C 1992 *Phys. Rev. B* **46** 6671
- [19] Monkhost H J and Pack J D 1976 *Phys. Rev. B* **13** 5188
- [20] Huber K P and Herzberg G 1979 *Molecular Spectra and Molecular Structure: IV. Constants of Diatomic Molecules* (New York: Van Nostrand-Reinhold) p 490
- [21] Otani M, Yamaguchi K, Miyagi H and Suzuki N 1998 *J. Phys.: Condens. Matter* **10** 11603